IEEE Access
Multidisciplinary | Rapid Review | Open Access Journal

Received 1 October 2023, accepted 17 October 2023, date of publication 30 October 2023, date of current version 3 November 2023.

Digital Object Identifier 10.1109/ACCESS.2023.3328641

RESEARCH ARTICLE

Enhancing Privacy-Preserving Personal Identification Through Federated Learning With Multimodal Vital Signs Data

TAE-HO HWANG, JINGYAO SHI, AND KANGYOON LEE, (Member, IEEE)
Department of Computer Engineering, Gachon University, Seongnam-si 13120, South Korea

Corresponding author: Kangyoon Lee (keylee@gachon.ac.kr)

This work was supported in part by the National Research Foundation of Korea under Grant NRF-2022R1F1A1069069; in part by the Korea Health Technology Research and Development Project through the Korea Health Industry Development Institute (KHIDI); and in part by the Ministry of Health & Welfare, Republic of Korea, under Grant HI22C1651.

ABSTRACT Personal identification (PI) can be verified using multimodal vital sign measurement methodologies in human physiology, such as electrocardiography (ECG) and radar signals. However, these processes are inevitably associated with concerns over privacy during the data collection and analysis stages, as well as discomfort during the physical measurement stages. To mitigate these issues, we explored the utilization of federated learning (FL) and noncontact sensors to ensure privacy protection and alleviate contact-related discomfort, respectively. Our objective was to establish the viability of privacy-secured PI models using FL. Furthermore, we examined the performance of FL-based PI models that incorporate non-contact radar signals, comparing the performance levels of five conventional machine learning (ML) models with those of five FL-based models using ECG and radar signals. Our experimental results indicate that although the ECG-based models exhibited superior overall accuracy, their radar-based counterparts demonstrated only slightly lower accuracy. These results confirm the effectiveness of FL-based PI models when compared with standard ML models. Thus, our study augments the evolution of privacy-guarded PI processes and lays a robust groundwork for future research in this field.

INDEX TERMS Bidirectional long short-term memory, ensemble model, electrocardiogram, federated learning, long short-term memory, personal identification, radar signals.

I. INTRODUCTION

The intersection of the fourth industrial revolution and changing population demographics has sparked a rapid proliferation of home and healthcare devices using the Internet of Things (IoT). In healthcare, there has been a notable shift from merely treating ailments to promoting overall wellness. Consequently, technologies that enable the continuous monitoring of vital signs within ambient-assisted living environments have gained significant importance owing to their capability to detect and predict health-related anomalies. These continuous monitoring processes are integral in platforms such as the Cognitive Health Advisor Platform [1].

Within multi-occupant environments, such as homes and offices, non-contact sensors (e.g., radar sensors) can be employed to measure vital signs. However, when a single radar sensor is used to randomly measure multiple individuals, personal identification (PI) is essential to monitor each individual distinctly.

Vital signs, such as electrocardiogram (ECG) data and radar signals, can be measured to verify PI. However, this approach presents several challenges. Specifically, privacy concerns are inevitably associated with the collection and analysis and personal data, and physical contact during measurements may lead to discomfort. Regulations such as the General Data Protection Regulation (GDPR), as well as federated learning (FL) techniques, can address and mitigate these privacy concerns, while the use of non-contact radar sensors can alleviate the discomfort associated with physical contact.

The associate editor coordinating the review of this manuscript and approving it for publication was Mansoor Ahmed.

Traditional vital sign measurement methods, such as ECG and photoplethysmography (PPG), require physical contact with the individual. The placement and adjustment of electrodes for these measurements can be intrusive by limiting movement and causing discomfort [2]. Conversely, although non-contact sensors – including radar, remote PPG (r-PPG) [3], [4], and infrared (IR) sensors – offer enhanced convenience, they may exhibit decreased accuracy owing to various noise factors. r-PPG sensors can measure parameters such as heart rate [5], respiration rate [6], and blood pressure [7], [8], whereas radar sensors can measure vital signs such as heart rate, respiration [9], [10], [11], [12], heart rate variability (HRV) [13], blood pressure [14], and movement patterns. Despite the aforementioned challenges, the use of vital signs for PI is becoming increasingly prevalence across multiple sectors including healthcare, security, and home appliances.

Although convolutional neural networks (CNNs) and long short-term memory (LSTM) networks are exceptionally effective for analyzing time-series data, such as ECG and radar signals, they require extensive data for training, which may further exacerbate privacy concerns in the context of personal information. FL represents a compelling solution to this problem, as it facilitates model training across devices without the need for data sharing, and subsequently sends model updates from each device to a central server. This process safeguards personal data from external exposure, allowing individuals to maintain control over their data while sharing collective insights to enhance model performance. Thus, the use of FL in tasks involving personal data, such as vital signs, simultaneously ensures the protection of privacy and improves model performance.

In this study, we employed FL-based algorithms to perform PI tasks on a cognitive health advisory platform. We compared the performance of FL models using radar signals (chosen for convenience in measurement) with those utilizing ECG signals. The objective of this study was to ascertain the viability of privacy-preserving FL-based models for PI. Furthermore, we investigated how the incorporation of non-contact radar signals impacts the performance of said models.

To achieve these objectives, we evaluated five machine learning (ML) models using ECG and radar signal data: CNN, LSTM, bidirectional LSTM (BLSTM), CNN-LSTM, and CNN-BLSTM. Furthermore, we implemented FL-based counterparts for the aforementioned ML models to evaluate and compare their performance on PI tasks. The performance evaluation incorporated the metrics of accuracy, precision, recall, and F1 score to determine the efficiency of conducting PI tasks while ensuring the protection of personal information [15].

This study makes several contributions to existing literature. First, we successfully demonstrated that high-accuracy PI tasks utilizing biometric signals can be performed while maintaining data privacy using FL-based models. This result reflects the potential of FL as a powerful tool for PI tasks, where data privacy is crucial. Furthermore, we confirmed the applicability of non-contact biosignals, particularly radar signal data, for use in PI models. This outcome indicates that FL can be instrumental in identifying individuals, particularly when contact-based methods are neither feasible nor preferable. Finally, we evaluated the performance of various PI models using two distinct types of data. These insights enrich the field of machine learning and offer practical value to researchers and practitioners in medicine and related fields.

The remainder of this paper is structured as follows. Section II outlines the methodology of the study. Section III describes the data preprocessing steps employed in this study, and offers a comparative accuracy analysis of the proposed models. Section IV presents insights based on a comparison with the results of previous studies. Finally, Section V presents concluding remarks and suggests potential future directions of research.

II. RELATED RESEARCH

A. METHODOLOGY

Biometric identification is based on unique physical or behavioral attributes of individuals, including fingerprints, irises, veins, and facial features [16]. Its applications span numerous fields such as access control, financial authentication, security, forensics, and the public sector. The use of vital signs in PI encompasses methods that use ECG [17], [18], [19], [20], [21], [22], [23], [24] and PPG [25].

ECG is a non-invasive method that employs simple skin-attached electrodes to measure signals. ECG encapsulates various components, such as the P wave, QRS complex, and T wave [26]. Various mathematical techniques can be used to analyze ECG signals, including signal processing, filtering, and pattern recognition. The Pan-Tompkins algorithm – which uses bandpass filtering, differentiation, squaring, moving-window integration, and thresholding – is commonly employed in ECG analysis to extract the QRS complex from signals.

Radar signals can be used to detect unique elements of human physiology including respiration, heartbeat, and movement. A raw radar signal is generated by emitting a wave and detecting the reflected signal using a radar sensor. The radar transceiver, which comprises a transmitter (Tx) and receiver (Rx), induces a phase shift in the reflected signal. This shift is proportional to the subtle movements of the chest surface stemming from cardiopulmonary activity [27], [28]. This approach does not require close contact with the individual and can automatically identify targets near the sensor, as well as significantly improving privacy compared to traditional measurement methods. Two methods for measuring vital signs using radar are ultrawideband (UWB) and frequency-modulated continuous waves (FMCW) [29], [30]. Overall, radar signals can be utilized for PI based on body shape and movement patterns [30].

B. PROPOSED MACHINE LEARNING MODEL ARCHITECTURE

CNN model architecture: The CNN is a machine learning architecture widely used for PI tasks. One-dimensional time-series ECG data were used in this study. CNNs are highly effective for ECG signal processing owing to their ability to discern complex patterns and unique features within each signal. Several prior studies have employed CNN models for PI tasks using ECG signals [31].

LSTM model architecture: The LSTM is a valuable architecture in the field of recurrent neural networks (RNNs), particularly for analyzing time-series ECG data [32]. An LSTM model includes a cell, input gate, output gate, and forget gate, which help adjust the input loss and prevent the vanishing gradient problem that often arises during backpropagation through time (BPTT) in RNNs [33], [34], [35]. The LSTM model constructed in this study included a filter size of 256 and three consecutive LSTM layers.

BLSTM model architecture: The bidirectional RNN architecture was developed to address issues encountered by traditional RNNs. A bidirectional RNN encompasses two types of recurrent networks—forward and backward—which are linked to generate output information with uniform measurements. These networks simultaneously handle both past and future information without experiencing delays over sequential timeframes. In the BLSTM architecture, two LSTM networks are trained for sequential inputs [36], [37], [38].

C. PROPOSED FEDERATED LEARNING-BASED MODEL ARCHITECTURE and FLOWER

1) FEDERATED LEARNING

FL represents an advanced form of machine learning designed to utilize data distributed across a multitude of clients without requiring direct data transfer between the clients and server [38]. Within the FL construct, a global model is retained on the server while each client trains a local model on individual data. These local model updates are shared with the global model, thereby enabling multitask learning, which in turn reduces communication costs [40]. An inherent feature of FL is that clients use local datasets and models for training, which offers a robust privacy shield that mitigates data leakage. Nonetheless, the applicability of FL can be hampered by several limiting factors such as sensitivity of personal information, unstable network conditions, restricted computational power, limited battery life, and limited storage [41], [42], [43].

Depending on the scale and nature of client participation, FL can be classified into two types: cross-device and cross-silo. Cross-device FL involves clients on a smaller scale, with each client possessing a minimal amount of local data. To achieve success in this setting, numerous edge devices were required throughout the training process. By contrast, clients in cross-silo FL are typically larger entities, such as corporations or institutions (e.g., hospitals and banks), while the participation count is smaller, with each client engaged in the complete learning process [44].

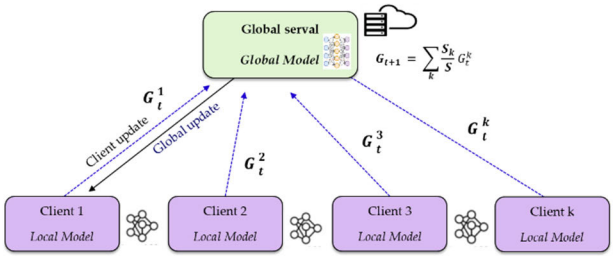

FIGURE 1. Example framework of proposed federated learning (FL) model and workflow of FL with k clients: 1. Download initial model parameters; 2. Train local models; 3. Upload local model parameters; 4. Secure aggregation of local models.

In this study, a PI model predicated on FL was constructed with four clients, with FL deployed to distinguish between home and office environments as single clients. The training procedure for the proposed FL method, illustrated in Figure 1 [45], commences with the server initializing the global model G_t and disseminating it to all k participating clients. Upon receiving G_t, each client trains it using its local data and returns an updated model to the server, with the returned models amalgamated to update the global model. This process is iteratively performed until the model reaches a state of convergence. The following formula is used for the updated global model:

$$G_{t+1} = \sum_k \frac{S_k}{S} G_t^k, \tag{1}$$

where S_k represents the number of training samples held by client k, and s denotes the total number of training samples across all clients.

2) FEDERATED LEARNING IMPLEMERENTATION PLATFORM: FLOWER

Various platforms and frameworks – including Flower [46], FedScale [47], FATE [48], PyShift [49], and EasyFL [50] – have been established to implement FL. Although the TensorFlow Federated (TFF) framework offers rudimentary FL capabilities based on TensorFlow [51], it requires the construction of a system for its application to an FL project. Both FedScale and EasyFL provide straightforward FL simulations using minimal code. However, these methods cannot easily be adapted to custom data or models, as they rely heavily on preexisting module codes and lack support for managing the lifecycles of FL operations. The latest iteration of the Flower platform, FLScalize [52], conveniently permits adjustments to the number of clients interacting with the server without requiring waiting periods between rounds. Notably, its outstanding client and server scheduling capabilities allow for effortless connectivity between servers and multiple clients to perform FL rounds, distinguishing it from other FL platforms. Accordingly, the Flower platform was selected to implement the proposed FL model in this study.

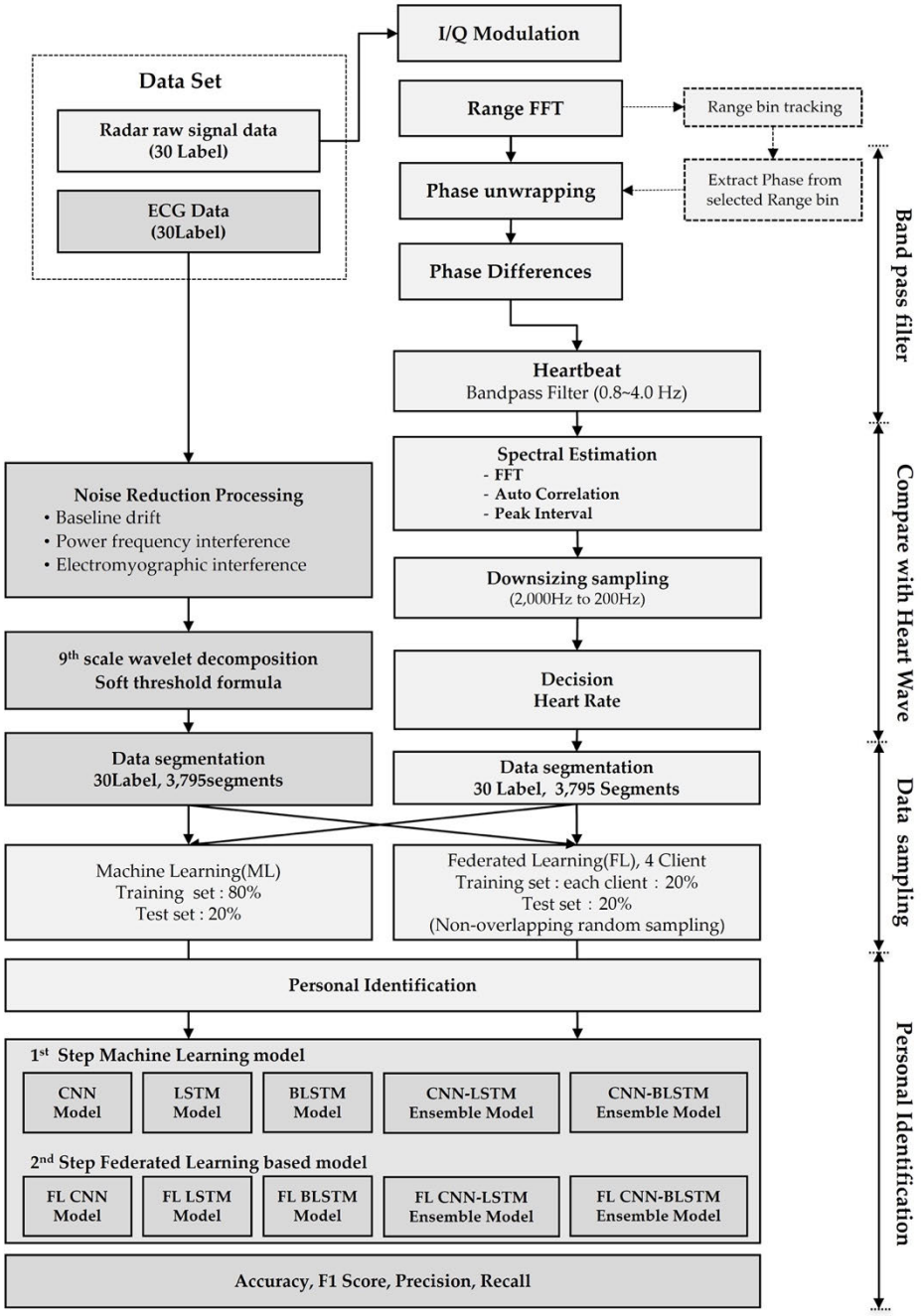

FIGURE 2. Process of implementing and comparing performance of personal identification models.

III. EXPERIMENTAL PRE-PROCESSING

The dataset used in this study included measurements obtained from 30 healthy participants—14 men and 16 women [53]—using a 24 GHz continuous-wave radar sensor. Data were collected using multiple synchronized reference sensors that simultaneously conducted electrocardiography (ECG), impedance cardiography, and non-invasive continuous blood pressure monitoring according to a predetermined protocol. This simultaneous data acquisition process helped reduce interference from other external factors, facilitating meaningful comparisons of the results.

The flowchart in Figure 2 briefly illustrates the experimental processes, including the separate preprocessing of ECG and radar data, training of each model, and verification.

A. ECG DATA PREPROCESSING

ECG data are typically vulnerable to various types of noise including power frequency interference [54],

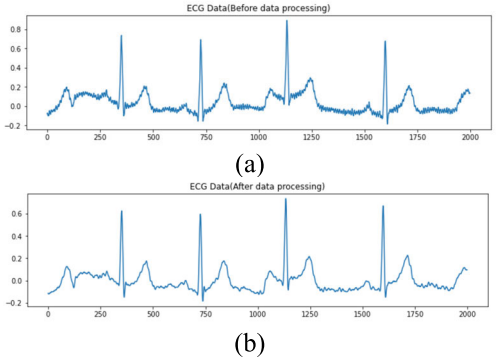

FIGURE 3. Comparison of electrocardiogram (ECG) data before (a) and after (b) noise filtering.

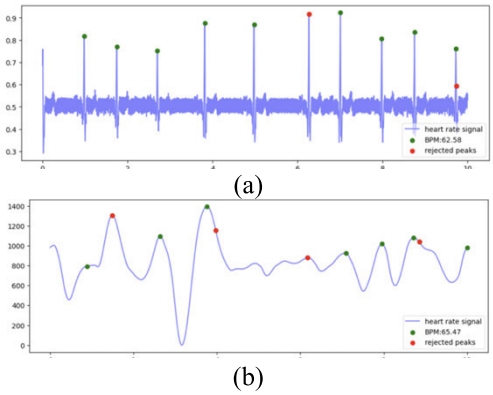

FIGURE 4. Illustration of peak detection in radar (a) and ECG (b) signals.

electromyographic interference, and baseline drift [55]. Several techniques, including wavelet transform [56], threshold filtering [57], and Fourier decomposition [58], have been explored to mitigate this vulnerability to noise. In the present study, ECG signals were initially sampled at a rate of 2,000 Hz and subsequently downsampled to 200 Hz. After performing a 9^{th}-order wavelet decomposition of the signals, the maximum frequency for the D1 level was set to 100 Hz. The coefficients of the D1 and D2 levels were discarded, whereas those of the D3-D9 levels were subjected to soft thresholding processing [59]. Figure 3 depicts results before and after noise filtering. Following segmentation, the ECG signal data were organized into 3,795 data segments, each associated with 30 data labels.

B. RADAR SIGNAL DATA PREPROCESSING

The raw radar signals captured in the database encapsulate multiple data types, including distance measurements, respiration rates, and heartbeats. The raw signals were segmented into I/Q (in-phase/quadrature) components and stored for further analysis. Digitization was performed at a sampling rate of 2,000 Hz. Owing to their raw nature, the signals were subjected to processing for PI purposes, specifically to isolate the required heartbeat signals.

To convert the raw radar signals into RF signals, we applied I/Q modulation as described in Equations (2)-(4):

$$A_c cos(\emptyset) = I \tag{2}$$

$$A_c sin(\emptyset) = Q \tag{3}$$

$$\boldsymbol{A_c cos(2\pi fct + \emptyset) = Icos\,(2\pi fct) - Q\,sin\,(2\pi fct)} \tag{4}$$

Following I/Q modulation, we employed FFT to ascertain the distance to the measured object. Subsequently, the respiratory and heartbeat signals were identified using band filtering.

The radar signals were downsampled from 2,000 Hz to 200 Hz to ensure an appropriate sampling interval between consecutive points within each heartbeat. Subsequently, each processed radar signal was divided into segments of 1,000 points each, approximately equivalent to 5 s of continuous data containing 6–9 heartbeats. Following segmentation, the radar signal data were divided into 3,795 data segments, each associated with 30 labels.

For validation, the processed radar signal data were compared with the simultaneously measured ECG reference data from the same individuals. A comparison was made by calculating the number of beats per minute (BPM) using the peak detection method for each signal type. The results shown in Figure 4 indicate that the separated signals obtained from the radar data closely correspond to the ECG-determined heartbeat signals.

Data were partitioned between training and test datasets. In conventional ML, data are generally split in an 80:20 ratio, with 80% of the data allocated for training and the remaining 20% reserved for testing. However, we adopted a different approach owing to the use of FL. Data were equitably distributed among the four clients, each receiving 20% of the data based on their respective subject matter, with no data duplication. The remaining 20% were set aside as test data. Leveraging the unique characteristics of FL ensures data privacy without requiring direct communication between clients, as communication is limited to interactions between servers and clients.

IV. RESULT

We evaluated and compared the performance of five ML-based and five FL-based PI models. These models were trained using both contact-based vital sign data, namely ECG data, and non-contact-based vital sign data derived from radar signals.

The CNN model comprises four convolutional layers. The first two of the three pooling layers are used for maximum pooling, with the last used for average pooling. Following feature extraction, the flattened layer is input to re-convert the content extracted by the convolutional layer into a one-dimensional vector. The final classification is performed using two fully-connected layers.

The LSTM model consists of three LSTM layers with 256 hidden state dimensions. Following the three LSTM layers, the dropout layer randomly sets the input elements to zero during the training process to minimize overfitting.

TABLE 1. Results of personal identification model training.

Dataset	Method	Model	Accuracy (%)	F1 Score (%)	Recall (Sensitivity) (%)	Specificity (%)	Precision (%)
ECG	Machine Learning	CNN	99.2	99.1	99.2	99.9	99.0
		LSTM	41.3	41.4	41.3	97.9	48.4
		BLSTM	44.5	44.2	44.5	98.0	46.6
		CNN-LSTM Ensemble	96.9	96.7	96.9	99.8	92.2
		CNN-BLSTM Ensemble	99.0	99.1	99.0	99.9	99.5
	Federated Learning	CNN	93.4	93.3	93.4	99.7	94.7
		LSTM	48.4	48.2	48.4	98.2	49.8
		BLSTM	49.2	48.6	49.2	98.2	50.0
		CNN-LSTM Ensemble	94.4	94.3	94.4	99.8	95.9
		CNN-BLSTM Ensemble	96.7	96.6	96.7	99.8	97.5
Radar Signals	Machine Learning	CNN	63.2	61.8	63.2	98.7	64.6
		LSTM	25.1	20.4	25.1	97.4	24.9
		BLSTM	28.0	24.4	28.0	97.5	29.1
		CNN-LSTM Ensemble	81.4	80.5	81.4	99.3	83.2
		CNN-BLSTM Ensemble	88.9	88.4	88.9	99.6	89.5
	Federated Learning	CNN	45.9	44.0	45.9	98.1	45.7
		LSTM	23.5	18.4	23.5	97.3	24.9
		BLSTM	29.3	25.4	29.3	97.5	28.1
		CNN-LSTM Ensemble	75.5	74.6	75.5	99.1	74.4
		CNN-BLSTM Ensemble	81.9	80.6	81.9	99.3	82.1

A drop rate of 0.2 was set to ensure that approximately 20% of the input elements were set to zero. The flattening layer is then used to flatten the multidimensional tensor into one dimension, followed by two fully-connected layers, and the final output represents prediction results for 30 categories.

Unlike the conventional LSTM architecture, a BLSTM model can process forward and backward sequence information simultaneously, thereby extracting more feature information. Otherwise, the two architectures are identical, except that the input and output sizes change between the second and third LSTM layers, enabling progressive feature extraction.

The CNN-LSTM/CNN-BLSTM model combines the strengths of the CNN and LSTM models. The CNN architecture is effective in extracting spatial features when processing input data, whereas the LSTM architecture is effective in extracting time-dependent features when processing sequential data. Consequently, the combined CNN-LSTM model can simultaneously capture spatiotemporal features in input data, which is desirable when processing radar signals.

As shown in Figures 5–8, the training curves of the LSTM and BLSTM models failed to converge, whereas those of the CNN model demonstrated successful convergence and yielded satisfactory results. This variation in performance may be attributed to the different processing capabilities of the aforementioned models. CNNs are effective in processing spatial features in images and 2D data. Therefore, if the data exhibit different local spatial patterns and characteristics, a CNN model can capture these properties more effectively, resulting in excellent convergence. In contrast, the LSTM and BLSTM models are better at handling time-series data and long-term dependencies. Because radar heartbeat signals encompass both temporal and spatial information, the CNN and LSTM models yield suboptimal results when used individually, and must instead be used in combination.

Based on these observations, we subsequently tested the combined CNN-LSTM and CNN-BLSTM models. The CNN layers were responsible for front-end feature extraction, whereas the LSTM/BLSTM layers further processed these features to harness the correlations inherent to time-series data. This integrated approach was better adapted to the data characteristics, thereby yielding enhanced performance.

The experimental results listed in Table 1 indicate that the CNN model achieved a high accuracy of 99.2% with the ECG dataset. Similarly, the CNN-LSTM and CNN-BLSTM models demonstrated acceptable accuracies of 96.9% and 99.0%, respectively. In terms of the FL-based models, the FL-CNN model achieved an accuracy of 93.4%, whereas the FL-CNN–LSTM and FL-CNN–BLSTM models exhibited high accuracies of 94.4% and 96.7%, respectively.

The aforementioned models exhibited different patterns when trained with radar signal data. The CNN model achieved an accuracy of 63.2%. However, performance significantly improved with the CNN-LSTM model, which achieved a higher accuracy of 81.4%, and the CNN-BLSTM model exhibited further improvement with an accuracy of 88.9%. In contrast, the FL-CNN model achieved a modest accuracy of 45.9%, whereas the FL-LSTM and FL-BLSTM models underperformed with accuracies of only 23.5% and 29.3%, respectively.

Despite these poor results, the FL-CNN-LSTM model yielded an accuracy of 75.5%, and the FL-CNN-BLSTM model exhibited an accuracy of 81.9%, demonstrating substantial improvements in performance.

Thus, the high accuracy attained by the FL-CNN-BLSTM model with ECG data marginally decreased when the model was applied to non-contact radar data. Receiver operating characteristic (ROC) curves corresponding to the eight models are presented in Appendix.

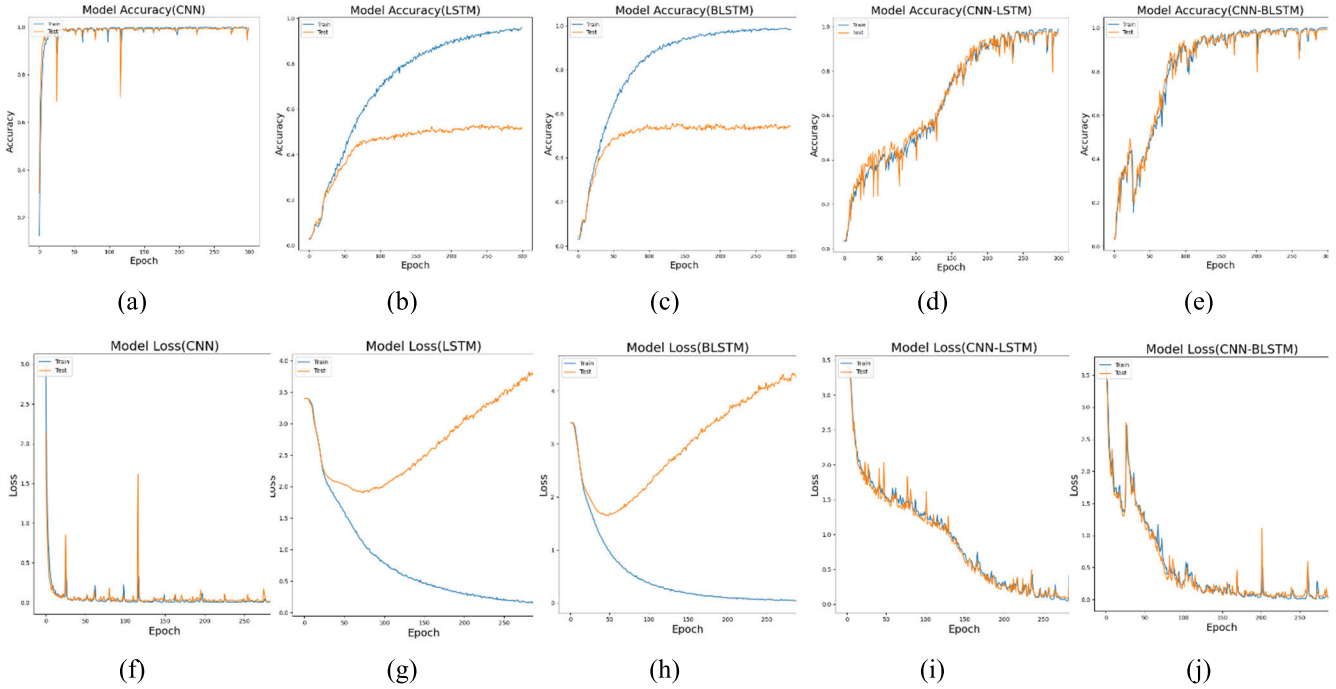

FIGURE 5. Training results of machine learning (ML)-based PI model using ECG data: accuracy and loss with increasing epochs. (a) CNN model accuracy; (b) LSTM model accuracy; (c) BLSTM model accuracy; (d) CNN-LSTM ensemble model accuracy; (e) CNN-BLSTM ensemble model accuracy; (f) CNN model loss; (g) LSTM model loss; (h) BLSTM model loss; (i) CNN-LSTM ensemble model loss; (j) CNN-BLSTM ensemble model loss.

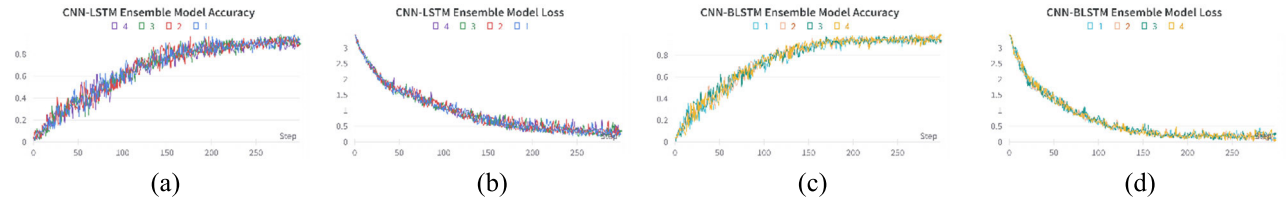

FIGURE 6. Results of FL-based personal identification model training using ECG data; accuracy and loss, as plotted with increasing epochs: (a) FL CNN model accuracy; (b) FL LSTM model accuracy; (c) FL BLSTM model accuracy; (d) FL CNN-LSTM ensemble model accuracy;.

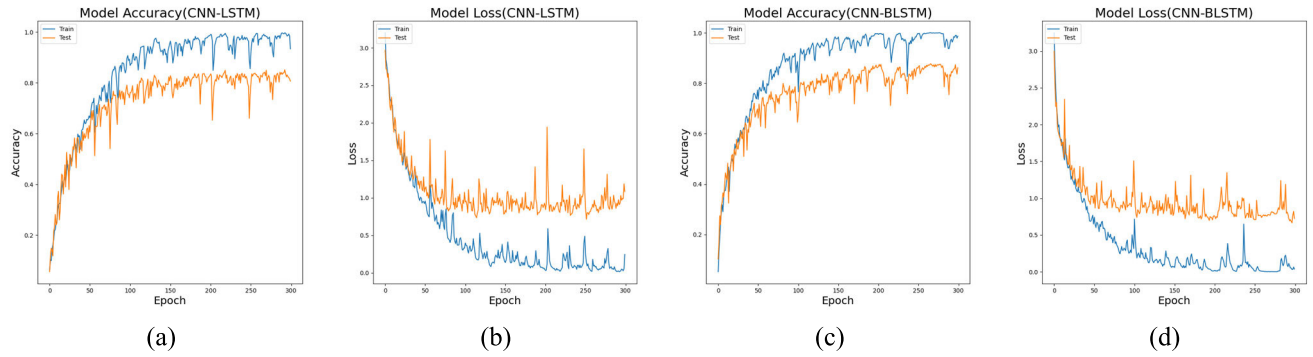

FIGURE 7. Results of the ML-based personal identification model training using radar signal data: accuracy and loss with increasing epochs. (a) CNN-LSTM ensemble model accuracy; (b) CNN-LSTM ensemble model loss; (c) BLTM ensemble model accuracy; (d) CNN-BLSTM ensemble model loss.

Overall, these results indicate that although contact-based ECG data yield more reliable individual recognition results when using the FL-CNN-BLSTM model, a reasonable level of accuracy is maintained when using non-contact radar data. This signifies the potential applicability of radar signals in situations where contact-based measurements are impractical,

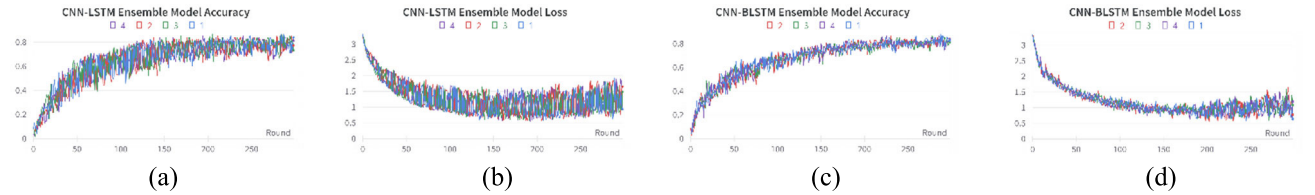

FIGURE 8. Results of the FL-based personal identification model training using radar signal data: accuracy and loss with increasing epochs. (a) FL CNN-LSTM ensemble model accuracy; (b) FL CNN-LSTM ensemble model loss; (c) FL CNN-BLSTM ensemble model accuracy; (d) FL CNN-BLSTM ensemble model loss.

TABLE 2. Personal recognition model training time.

Dataset	Method	Model	Time	Dataset	Method	Model	Time
ECG	Machine Learning	CNN	2min 13.0sec	Radar Signals	Machine Learning	CNN	2min 14.0sec
		LSTM	2min 6.0sec			LSTM	2min 12.5sec
		BLSTM	2min 25.7sec			BLSTM	2min 28.4sec
		CNN-LSTM Ensemble	6min 25.9sec			CNN-LSTM Ensemble	6min 31.0sec
		CNN-BLSTM Ensemble	6min 27.0sec			CNN-BLSTM Ensemble	6min 28.2sec
	Federated Learning	CNN	4min 18.0sec		Federated Learning	CNN	4min 29.0sec
		LSTM	5min 9.8sec			LSTM	5min 22.0sec
		BLSTM	6min 58.2sec			BLSTM	7min 14.5sec
		CNN-LSTM Ensemble	12min 40.5sec			CNN-LSTM Ensemble	12min 49.0sec
		CNN-BLSTM Ensemble	12min 47.5sec			CNN-BLSTM Ensemble	12min 57.6sec

TABLE 3. Comparison of proposed method with recent state-of-the-art methods in terms of classification accuracy of four classes.

Dataset	Method		Model	Accuracy (%)	F1 Score (%)	Recall (Sensitivity) (%)	Specificity (%)
MIT-BIH ECG	Lynn et al. [22]		BLSTM	99.5	99.2	99.2	98.8
	Zhang et al. [60]		1D-CNN	98.6	92.2	95.2	97.3
	Mostayed et al. [61]		LSTM	99.4	96.8	95.8	99.7
	Zabir Al et al. [62]		LSTM	80.1	83.59	82.8	89.1
	Fan Liu et al. [63]		LSTM-CNN	80.1	83.59	82.8	89.1
	Proposed	Machine Learning	CNN-LSTM Ensemble	97.6	97.5	97.6	99.9
			CNN-BLSTM Ensemble	98.2	98.2	98.2	99.9
		Federated Learning	CNN-LSTM Ensemble	96.8	96.8	96.8	99.9
			CNN-BLSTM Ensemble	97.3	97.3	97.3	99.9
ECG Signals	Proposed	Machine Learning	CNN-LSTM Ensemble	96.9	96.7	96.9	99.8
			CNN-BLSTM Ensemble	99.0	99.1	99.0	99.9
		Federated Learning	CNN-LSTM Ensemble	94.4	94.3	94.4	99.8
			CNN-BLSTM Ensemble	96.7	96.6	96.7	99.8
Radar Signals	Proposed	Machine Learning	CNN-LSTM Ensemble	81.4	80.5	81.4	99.3
			CNN-BLSTM Ensemble	88.9	88.4	88.9	99.6
		Federated Learning	CNN-LSTM Ensemble	75.5	74.6	75.5	99.1
			CNN-BLSTM Ensemble	81.9	80.6	81.9	99.3

such as office environments. These findings also underscore the potential of FL as a tool for individual recognition using biometric signals, thereby offering a privacy-preserving solution suitable for practical applications

In terms of training efficiency, the average training time of the CNN/LSTM/BLSTM models in the GPU 3090 environment was 2 min 10sec, whereas that of the CNN-LSTM/CNN-BLSTM models was 6 min. Furthermore, the FL-CNN/FL-LSTM/FL-BLSTM models in this environment required an average training time of 4 min 10sec, whereas the FL-CNN-LSTM/FL-CNN-BLSTM models required an average training time of 12 min. The increases in training time may be attributed to the increased efficiency of communication between the client and server.

V. DISCUSSION

As listed in Table 3, the findings of this study are comparable to or surpass those of previous studies in terms of accuracy. For instance, earlier studies utilizing ECG (MIT-BIH) data reported accuracies ranging from 80.1% to 99.5% [23], [60], [61], [62], [63]. In contrast, our study achieved an impressive accuracy of 98.2% using the CNN-BLSTM model for ECG data. Similarly, we achieved a notable accuracy of 88.9% for radar signal data with the CNN-BLSTM model,

TABLE 4. Performance evaluation of radar-signal-based personal recognition model under different motion states.

Dataset	Method	Model	State	Accuracy (%)	F1 Score (%)	Recall (Sensitivity) (%)	Specificity (%)
Radar Signals	Federated Learning	CNN-LSTM Ensemble	Resting	75.5	74.6	75.55	99.1
			Valsalva	69.4	68.8	69.4	98.9
			Apnea	42.6	41.8	42.6	98.5
			Random Mix	81.3	81.2	81.3	99.3
		CNN-BLSTM Ensemble	Resting	81.9	80.6	81.9	99.3
			Valsalva	74.6	74.3	74.6	99.1
			Apnea	45.7	43.6	45.7	98.5
			Random Mix	82.1	81.9	82.1	99.3

surpassing the 80.1% accuracy reported in a previous study on ECG-based personal identification by Zabir et al. Additionally, the FL-CNN-BLSTM model demonstrated an accuracy of 81.9%, which was consistent with the results of a previous study. Overall, the models developed in this study demonstrated effectiveness in performing PI tasks using vital sign data.

Radar signal data inherently contain noise owing to motion during measurement, and noisy spatial features may remain even after filtering, potentially influencing classification accuracy. To examine the impact of respiratory motion on model performance, we defined four measurement states – resting, Valsalva, apnea, and random mix – and compared individual recognition capabilities of the for each state. According to the results presented in Table 4, classification accuracy was higher for the resting and random mixed states, and lower for the Valsalva and apnea states.

VI. CONCLUSION

In this study, we compared PI performance using contact and non-contact biometric signals, namely ECG and radar data, respectively. Five ML and five FL models were evaluated in terms of accuracy and F1 score. Our findings indicate that contact signals are more effective for PI tasks than non-contact signals. Nevertheless, the results highlight the potential of FL-based models that utilize non-contact vital signs, such as radar signal data, as a practical and privacy-preserving solution for PI considering user convenience.

Although this study demonstrated promising potential for non-contact biometric-based PI, several aspects require further investigation. First, the sample size of the non-contact dataset was relatively small compared with that of the contact dataset, which impacted the accuracy and generalizability of the results. Future research should explore methods to enhance accuracy by employing multiple non-contact biometric signals and larger sample sizes. In addition, although FL has the potential to enhance PI protection, it can be further refined and optimized. Future studies should therefore focus on developing more sophisticated FL algorithms to effectively handle distributed data and computational challenges while addressing the personalization aspects of FL.

The results of this study provide strong support for the applicability of contactless biometric signals across multiple fields to improve data protection and enhance user convenience.

To strengthen the protection of personal information, the integration of contactless biometric signals and federated learning provides a more convenient and privacy-protecting method for personal identification. Contactless identification methods can be expected to increase user comfort while ensuring a sufficient degree of privacy.

Overall, we expect future studies to drive innovation and progress in this field. We will also continue to conduct research with the objectives of expanding the sample size of contactless data to enhance model accuracy, and improving the handling of distributed data to protect personalized information.

APPENDIX

Appendix A: ROC evaluation of the two ensemble models using ECG and radar data in general machine learning methods (ML) and federated learning methods (FL).

REFERENCES

[1] K. Lee, "Reference model and architecture of interactive cognitive health advisor based on evolutional cyber-physical systems," *KSII Trans. Internet Inf. Syst.*, vol. 13, no. 8, pp. 4270–4284, Aug. 2019.
[2] A. K. Sowan, A. F. Tarriela, T. M. Gomez, C. C. Reed, and K. M. Rapp, "Nurses' perceptions and practices toward clinical alarms in a transplant cardiac intensive care unit: Exploring key issues leading to alarm fatigue," *JMIR Hum. Factors*, vol. 2, no. 1, p. e3, Jan./Jun. 2015, doi: 10.2196/humanfactors.4196.
[3] M. Lewandowska, J. Ruminski, T. Kocejko, and J. Nowak, "Measuring pulse rate with a webcam—A non-contact method for evaluating cardiac activity," in *Proc. Federated Conf. Comput. Sci. Inf. Syst. (FedCSIS)*, Szczecin, Poland, Sep. 2011, pp. 405–410.
[4] H. E. Tasli, A. Gudi, and M. den Uyl, "Remote PPG based vital sign measurement using adaptive facial regions," in *Proc. IEEE Int. Conf. Image Process. (ICIP)*, Paris, France, Oct. 2014, pp. 1410–1414, doi: 10.1109/ICIP.2014.7025282.
[5] A. Ni, A. Azarang, and N. Kehtarnavaz, "A review of deep learning-based contactless heart rate measurement methods," *Sensors*, vol. 21, no. 11, p. 3719, May 2021, doi: 10.3390/s21113719.
[6] J. Du, S. -Q. Liu, B. Zhang, and P. C. Yuen, "Weakly supervised rppg estimation for respiratory rate estimation," in *Proc. IEEE/CVF Int. Conf. Comput. Vis. Workshops (ICCVW)*, Montreal, BC, Canada, 2021, pp. 2391–2397, doi: 10.1109/ICCVW54120.2021.00271.
[7] F. Schrumpf, P. Frenzel, C. Aust, G. Osterhoff, and M. Fuchs, "Assessment of non-invasive blood pressure prediction from PPG and rPPG signals using deep learning," *Sensors*, vol. 21, no. 18, p. 6022, Sep. 2021, doi: 10.3390/s21186022.

[8] S. Ghosh, A. Banerjee, N. Ray, P. W. Wood, P. Boulanger, and R. Padwal, "Continuous blood pressure prediction from pulse transit time using ECG and PPG signals," in *Proc. IEEE Healthcare Innov. Point-Care Technol. Conf. (HI-POCT)*, Cancun, Mexico, Nov. 2016, pp. 188–191, doi: 10.1109/HIC.2016.7797728.

[9] J. Liu, K. Zhang, W. He, J. Ma, L. Peng, and T. Zheng, "Non-contact human fatigue assessment system based on millimeter wave radar," in *Proc. IEEE 4th Int. Conf. Electron. Technol. (ICET)*, Chengdu, China, May 2021, pp. 173–177, doi: 10.1109/ICET51757.2021.9451149.

[10] A. Tekleab and M. Sanduleanu, "Vital signs detection using FMCW radar," in *Proc. Int. Conf. Electr. Comput. Technol. Appl. (ICECTA)*, Ras Al Khaimah, United Arab Emirates, Nov. 2022, pp. 51–54, doi: 10.1109/ICECTA57148.2022.9990258.

[11] L. Ren, Y. S. Koo, Y. Wang, and A. E. Fathy, "Noncontact heartbeat detection using UWB impulse Doppler radar," in *Proc. IEEE Topical Conf. Biomed. Wireless Technol., Netw., Sens. Syst. (BioWireleSS)*, San Diego, CA, USA, Jan. 2015, pp. 1–3, doi: 10.1109/BIOWIRELESS.2015.7152128.

[12] C. Will, K. Shi, S. Schellenberger, T. Steigleder, F. Michler, R. Weigel, C. Ostgathe, and A. Koelpin, "Local pulse wave detection using continuous wave radar systems," *IEEE J. Electromagn., RF Microw. Med. Biol.*, vol. 1, no. 2, pp. 81–89, Dec. 2017, doi: 10.1109/JERM.2017.2766567.

[13] E. Al-Masri and M. Momin, "Detecting heart rate variability using millimeter-wave radar technology," in *Proc. IEEE Int. Conf. Big Data (Big Data)*, Seattle, WA, USA, Dec. 2018, pp. 5282–5284, doi: 10.1109/BigData.2018.8622096.

[14] M. Jung, M. Caris, and S. Stanko, "Non-contact blood pressure estimation using a 300 GHz continuous wave radar and machine learning models," in *Proc. IEEE Int. Symp. Med. Meas. Appl. (MeMeA)*, Lausanne, Switzerland, Jun. 2021, pp. 1–6, doi: 10.1109/MeMeA52024.2021.9478734.

[15] H. Dalianis, "Evaluation metrics and evaluation," in *Clinical Text Mining*. Cham, Switzerland: Springer, 2018, pp. 45–53.

[16] A. K. Jain, A. Ross, and S. Prabhakar, "An introduction to biometric recognition," *IEEE Trans. Circuits Syst. Video Technol.*, vol. 14, no. 1, pp. 4–20, Jan. 2004, doi: 10.1109/TCSVT.2003.818349.

[17] L. Biel, O. Pettersson, L. Philipson, and P. Wide, "ECG analysis: A new approach in human identification," *IEEE Trans. Instrum. Meas.*, vol. 50, no. 3, pp. 808–812, Jun. 2001, doi: 10.1109/19.930458.

[18] F. Sufi, I. Khalil, and J. Hu, "ECG-based authentication," in *Handbook of Infor-Mation and Communication Security*, P. Stavroulakis and M. Stamp, Eds. Berlin, Germany: Springer, 2010.

[19] S. Asadianfam, M. J. Talebi, and E. Nikougoftar, "ECG modelling using wavelet networks: Application to biometrics," *Int. J. Bi-Ometrics*, vol. 2, no. 3, pp. 236–249, 2010.

[20] J. Pinto, J. Cardoso, A. Lourenço, and C. Carreiras, "Towards a continuous biometric system based on ECG signals acquired on the steering wheel," *Sensors*, vol. 17, no. 10, p. 2228, Sep. 2017, doi: 10.3390/s17102228.

[21] D. Wang, Y. Si, W. Yang, G. Zhang, and J. Li, "A novel electrocardiogram biometric identification method based on temporal-frequency autoencoding," *Electronics*, vol. 8, no. 6, p. 667, Jun. 2019, doi: 10.3390/electronics8060667.

[22] A. E. Ibrahim, S. Abdel-Mageid, N. Nada, and M. A. Elshahed, "ECG signals for human identification based on fiducial and non-fiducial approaches," *Int. J. Adv. Comput. Res.*, vol. 10, no. 47, pp. 89–95, Mar. 2020, doi: 10.19101/IJACR.2019.940129.

[23] H. M. Lynn, P. Kim, and S. B. Pan, "Data independent acquisition based bi-directional deep networks for biometric ECG authentication," *Appl. Sci.*, vol. 11, no. 3, p. 1125, Jan. 2021, doi: 10.3390/app11031125.

[24] S. Hamza and Y. B. Ayed, "Toward improving person identification using the ElectroCardioGram (ECG) signal based on non-fiducial features," *Multimedia Tools Appl.*, vol. 81, no. 13, pp. 18543–18561, May 2022, doi: 10.1007/s11042-022-12244-0.

[25] N. Karimian, Z. Guo, M. Tehranipoor, and D. Forte, "Human recognition from photoplethysmography (PPG) based on non-fiducial features," in *Proc. IEEE Int. Conf. Acoust., Speech Signal Process. (ICASSP)*, New Or-leans, LA, USA, Mar. 2017, pp. 4636–4640, doi: 10.1109/ICASSP.2017.7953035.

[26] H. Li and P. Boulanger, "A survey of heart anomaly detection using ambulatory electrocardiogram (ECG)," *Sensors*, vol. 20, no. 5, p. 1461, Mar. 2020, doi: 10.3390/s20051461.

[27] C. Li, V. M. Lubecke, O. Boric-Lubecke, and J. Lin, "A review on recent advances in Doppler radar sensors for noncontact healthcare monitoring," *IEEE Trans. Microw. Theory Techn.*, vol. 61, no. 5, pp. 2046–2060, May 2013, doi: 10.1109/TMTT.2013.2256924.

[28] S. H. Choi and H. Yoon, "Convolutional neural networks for the real-time monitoring of vital signs based on impulse radio ultrawide-band radar during sleep," *Sensors*, vol. 23, no. 6, p. 3116, Mar. 2023, doi: 10.3390/s23063116.

[29] C. Wolff. (2018). *Radar Basics*. [Online]. Available: http://radartutorial.eu/02.basics/Frequency%20Modulated%20Continuous%20Wave%20Radar.en.html

[30] T. Sakamoto, "Personal identification using ultrawideband radar measurement of walking and sitting motions and a convolutional neural network," Aug. 2020, *arXiv:2008.02182*.

[31] J. Xu, T. Li, Y. Chen, and W. Chen, "Personal identification by convolutional neural network with ECG signal," in *Proc. Int. Conf. Inf. Commun. Technol. Converg. (ICTC)*, Jeju, South Korea, Oct. 2018, pp. 559–563, doi: 10.1109/ICTC.2018.8539632.

[32] S. Hochreiter and J. Schmidhuber, "Long short-term memory," *Neural Comput.*, vol. 9, no. 8, pp. 1735–1780, Nov. 1997, doi: 10.1162/neco.1997.9.8.1735.

[33] H. I. Fawaz, G. Forestier, J. Weber, L. Idoumghar, and P.-A. Müller, "Deep learning for time series classification: A review," *Data Mining Knowl. Discovery*, vol. 33, no. 4, pp. 917–963, Jul. 2019, doi: 10.1007/s10618-019-00619-1.

[34] B.-H. Kim and J.-Y. Pyun, "ECG identification for personal authentication using LSTM-based deep recurrent neural networks," *Sensors*, vol. 20, no. 11, p. 3069, May 2020, doi: 10.3390/s20113069.

[35] J.-A. Lee and K.-C. Kwak, "Personal identification using an ensemble approach of 1D-LSTM and 2D-CNN with electrocardiogram signals," *Appl. Sci.*, vol. 12, no. 5, p. 2692, Mar. 2022, doi: 10.3390/app12052692.

[36] M. Schuster and K. K. Paliwal, "Bidirectional recurrent neural networks," *IEEE Trans. Signal Process.*, vol. 45, no. 11, pp. 2673–2681, Nov. 1997, doi: 10.1109/78.650093.

[37] Ö. Yildirim, "A novel wavelet sequence based on deep bidirectional LSTM network model for ECG signal classification," *Comput. Biol. Med.*, vol. 96, pp. 189–202, May 2018, doi: 10.1016/j.compbiomed.2018.03.016.

[38] H. Abrishami et al., "Supervised ECG interval segmentation using LSTM neural network," in *Proc. Int. Conf. Bioinf. Comput. Biol., Steering Committee World Congr. Comput. Sci., Comput. Eng. Applied Comput. (BIOCOMP/WorldComp)*, 2018, pp. 71–77.

[39] T. Zhang, L. Gao, C. He, M. Zhang, B. Krishnamachari, and A. S. Avestimehr, "Federated learning for the Internet of Things: Applications, challenges, and opportunities," *IEEE Internet Things Mag.*, vol. 5, no. 1, pp. 24–29, Mar. 2022, doi: 10.1109/IOTM.004.2100182.

[40] R. Shokri and V. Shmatikov, "Privacy-preserving deep learning," in *Proc. 53rd Annu. Allerton Conf. Commun., Control, Comput. (Allerton)*, Sep. 2015, pp. 1310–1321.

[41] J. Konečný, H. B. McMahan, D. Ramage, and P. Richtárik, "Federated optimization: Distributed machine learning for on-device intelligence," 2016, *arXiv:1610.02527*.

[42] J. Konečný, H. B. McMahan, F. X. Yu, P. Richtárik, A. T. Suresh, and D. Bacon, "Federated learning: Strategies for improving communication efficiency," 2016, *arXiv:1610.05492*.

[43] J. Konečný, B. McMahan, and D. Ramage, "Federated optimization: Distributed optimization beyond the datacenter," 2015, *arXiv:1511.03575*.

[44] C. Huang, J. Huang, and X. Liu, "Cross-silo federated learning: Challenges and opportunities," 2022, *arXiv:2206.12949*.

[45] Y. Gao, M. Kim, S. Abuadbba, Y. Kim, C. Thapa, K. Kim, S. A. Camtepe, H. Kim, and S. Nepal, "End-to-end evaluation of federated learning and split learning for Internet of Things," 2020, *arXiv:2003.13376*.

[46] D. J. Beutel, T. Topal, A. Mathur, X. Qiu, J. Fernandez-Marques, Y. Gao, L. Sani, K. H. Li, T. Parcollet, P. P. Buarque de Gusmão, and N. D. Lane, "Flower: A friendly federated learning framework," Mar. 2022, doi: 10.48550/arXiv.2007.14390.

[47] F. Lai, Y. Dai, S. Singapuram, J. Liu, X. Zhu, H. Madhyastha, and M. Chowdhury, "Fedscale: Benchmarking model and system performance of federated learning at scale," in *Proc. Int. Conf. Mach. Learn.*, 2022, pp. 11814–11827.

[48] Y. Liu et al., "FATE: An industrial grade platform for collaborative learning with data protection," *J. Mach. Learn. Res.*, vol. 22, no. 226, pp. 1–6, 2021.

[49] J. Xie, K. Zhang, and A. T. Frank, "PyShifts: A PyMOL plugin for chemical shift-based analysis of biomolecular ensembles," *J. Chem. Inf. Model.*, vol. 60, no. 3, pp. 1073–1078, Mar. 2020, doi: 10.1021/acs.jcim.9b01039.

[50] W. Zhuang, X. Gan, Y. Wen, and S. Zhang, "EasyFL: A low-code federated learning platform for dummies," *IEEE Internet Things J.*, vol. 9, no. 15, pp. 13740–13754, Aug. 2022, doi: 10.1109/JIOT.2022.3143842.

[51] I. Kholod, E. Yanaki, D. Fomichev, E. Shalugin, E. Novikova, E. Filippov, and M. Nordlund, "Open-source federated learning frameworks for IoT: A comparative review and analysis," *Sensors*, vol. 21, no. 1, p. 167, Dec. 2020, doi: 10.3390/s21010167.
[52] S. Yang, J. Moon, J. Kim, K. Lee, and K. Lee, "FLScalize: Federated learning lifecycle management platform," *IEEE Access*, vol. 11, pp. 47212–47222, 2023, doi: 10.1109/ACCESS.2023.3275439.
[53] S. Schellenberger, K. Shi, T. Steigleder, A. Malessa, F. Michler, L. Hameyer, N. Neumann, F. Lurz, R. Weigel, C. Ostgathe, and A. Koelpin, "A dataset of clinically recorded radar vital signs with synchronised reference sensor signals," *Sci. Data*, vol. 7, no. 1, p. 291, Sep. 2020, doi: 10.1038/s41597-020-00629-5.
[54] M. Niegowski, M. Zivanovic, M. Gómez, and P. Lecumberri, "Unsupervised learning technique for surface electromyogram denoising from power line interference and baseline wander," in *Proc. Annu. Int. Conf. IEEE Eng. Med. Biol. Soc., 37th Annu. Int. Conf. IEEE Eng. Med. Biol. Soc. (EMBC)*, Milan, Italy, Aug. 2015, pp. 7274–7277, doi: 10.1109/EMBC.2015.7320071.
[55] C. Wu, Y. Zhang, C. Hong, and H. Chiueh, "Implementation of ECG signal processing algorithms for removing baseline wander and electromyography interference," in *Proc. 8th IEEE Int. Conf. Commun. Softw. Netw. (ICCSN)*, Beijing, China, Jun. 2016, pp. 118–121.
[56] N. Rashmi, G. Begum, and V. Singh, "ECG denoising using wavelet transform and filters," in *Proc. Int. Conf. Wireless Commun., Signal Process. Netw. (WiSPNET)*, Chennai, India, Mar. 2017, pp. 2395–2400, doi: 10.1109/WiSPNET.2017.8300189.
[57] W. Jenkal, R. Latif, A. Toumanari, A. Dliou, O. El B'charri, and F. M. R. Maoulainine, "An efficient algorithm of ECG signal denoising using the adaptive dual threshold filter and the discrete wavelet transform," *Biocybernetics Biomed. Eng.*, vol. 36, no. 3, pp. 499–508, 2016, doi: 10.1016/j.bbe.2016.04.001.
[58] A. Singhal, P. Singh, B. Fatimah, and R. B. Pachori, "An efficient removal of power-line interference and baseline wander from ECG signals by employing Fourier decomposition technique," *Biomed. Signal Process. Control*, vol. 57, Mar. 2020, Art. no. 101741, doi: 10.1016/j.bspc.2019.101741.
[59] D. L. Donoho, "De-noising by soft-thresholding," *IEEE Trans. Inf. Theory*, vol. 41, no. 3, pp. 613–627, May 1995, doi: 10.1109/18.382009.
[60] Q. Zhang, D. Zhou, and X. Zeng, "HeartID: A multiresolution convolutional neural network for ECG-based biometric human identification in smart health applications," *IEEE Access*, vol. 5, pp. 11805–11816, 2017, doi: 10.1109/ACCESS.2017.2707460.
[61] A. Mostayed, J. Luo, X. Shu, and W. Wee, "Classification of 12-lead ECG signals with bi-directional LSTM network," 2018, *arXiv:1811.02090*.
[62] Z. A. Nazi, A. Biswas, M. A. Rayhan, and T. A. Abir, "Classification of ECG signals by dot residual LSTM network with data augmentation for anomaly detection," in *Proc. 22nd Int. Conf. Comput. Inf. Technol. (ICCIT)*, Dec. 2019, pp. 1–5.
[63] F. Liu, X. Zhou, T. Wang, J. Cao, Z. Wang, H. Wang, and Y. Zhang, "An attention-based hybrid LSTM-CNN model for arrhythmias classification," in *Proc. Int. Joint Conf. Neural Netw. (IJCNN)*, Jul. 2019, pp. 1–8, doi: 10.1109/IJCNN.2019.8852037.

TAE-HO HWANG received the B.S. degree in nuclear engineering and mechanical engineering and the M.B.A. and M.S. degrees from Hanyang University, Seoul, South Korea, in 1985 and 1991, respectively. He is currently pursuing the Ph.D. degree with the Cognitive Computing Laboratory, Department of Computer Engineering, Gachon University. Previously, he was a System Engineer with Samsung Electronics, from 1985 to 1991. His research interests include big data, the IoT, artificial intelligence, and deep learning.

JINGYAO SHI received the bachelor's degree from Gachon University, Seongnam-si, South Korea, in 2019, where he is currently pursuing the Ph.D. degree with the Department of Computer Engineering. His research interests include healthcare, the IoT open platforms, artificial intelligence, and sensor development.

KANGYOON LEE (Member, IEEE) received the B.S. degree in electronics engineering and the M.S. degree in computer science from Yonsei University, Seoul, South Korea, in 1986 and 1996, respectively, and the Ph.D. degree in IT policy management from Soongsil University, Seoul, in 2010. From 2008 to 2014, he was the Director of the IBM Korea Laboratory for Ubiquitous Computing and Software Solutions. In 2014, he was promoted to the Leader of the IBM Watson Business Unit, South Korea. Since 2016, he has been a Professor with the Computer Engineering Department, IT College, Gachon University. He has been the Director of the Gachon Artificial Intelligence Technology Center, since 2016. His research interests include cognitive computing, healthcare advisory, the IoT platforms, and industry transformation.